Domain and crystal structure of superconducting $Ba_2YCu_3O_{8-\delta}$ at 40 and 100 K by single-crystal neutron diffraction

G. J. McIntyre*
Institut Laue-Langevin, 156X, 38042 Grenoble Cedex, France

A. Renault†
Laboratoire de Physique des Solides, Bâtiment 510, Université de Paris-Sud, 91405 Orsay, France

G. Collin
Université René Déscartes, 4 Avenue de l'Observatoire, 75006 Paris, France
(Received 5 November 1987)

The domain and crystal structure of orthorhombic $Ba_2YCu_3O_{8-\delta}$ ($\delta \simeq 1.30$) has been investigated at 40 and 100 K by single-crystal neutron diffraction. As the crystals were cooled from the tetragonal growth phase the reciprocal lattice split quadruply due to interchange of the orthorhombic *a* and *b* axes on a macroscopic scale and to microscopic twinning about (110) planes. Recording the diffraction pattern on a multidetector allowed some separation of the individual orthorhombic reflections. The intensity ratios of the individual reflections of some split peaks are shown to be particularly sensitive to the relative occupations of the oxygen sites in the plane between pairs of closest Ba atoms, and confirm that the oxygen lies on just one site. Large thermal parameters are observed for the copper and oxygen atoms in the chains of corner-linked CuO_4 groups.

I. INTRODUCTION

The observation by Wu *et al.*[1] of superconductivity above 90 K in a mixed-phase compound of the Ba-Y-Cu-O system has sparked frenetic activity in many laboratories to identify and characterize the specific phase responsible for the high-temperature superconductivity. From studies of the Ba-Y-Cu-O phase diagram using powder diffraction and transport measurements, Rao *et al.*[2] and Hinks *et al.*[3] concluded that the superconducting material is single phase with composition $Ba_2YCu_3O_{8-\delta}$. The exact oxygen stoichiometry determines the ratio of the number of copper atoms with formal charge 2+ to the number with formal charge 3+, which in turn seems to govern the occurrence of high-temperature superconductivity.[4]

The structure is also very sensitive to the oxygen stoichiometry. The early x-ray determinations of these structures were somewhat inconclusive as to the oxygen positions and occupations due to the low scattering power of x rays by oxygen compared to barium, yttrium, and copper, and, in some cases, due also to twinning of the samples.[5-7] It has now been well established by neutron powder diffraction that the structure of the superconducting phase is orthorhombic with space group *Pmmm*.[8-13] Most of the oxygen atoms are located on four sets of sites. If we adopt the nomenclature of Ref. 5 (see Fig. 1), the sites O(1), O(2), and O(3) appear to be nearly fully occupied, while the site O(5) at $(\frac{1}{2},0,0)$ appears to be completely empty at room temperature. The occupation of O(4) at $(0,\frac{1}{2},0)$ adjusts to the oxygen stoichiometry; $Ba_2YCu_3O_7$ corresponds to full occupation of O(4). A notable consequence of the (nearly) full occupation of O(4) and the absence of oxygen at O(5) is the bonding of sheets of nearly square-planar corner-linked CuO_4 groups by chains of planar CuO_4 groups oriented in the *b*-*c* plane and linked along the *b* axis. Apart from the differences in the O(4) and O(5) occupations the structure is remarkably close to tetragonal. The *a* and *b* lattice parameters at room temperature differ by only 0.06 Å, and the *z* coordinates of O(2) and O(3) at $(\frac{1}{2},0,z)$ and $(0,\frac{1}{2},z)$, respectively, which like O(4) and O(5) would be crystallograph-

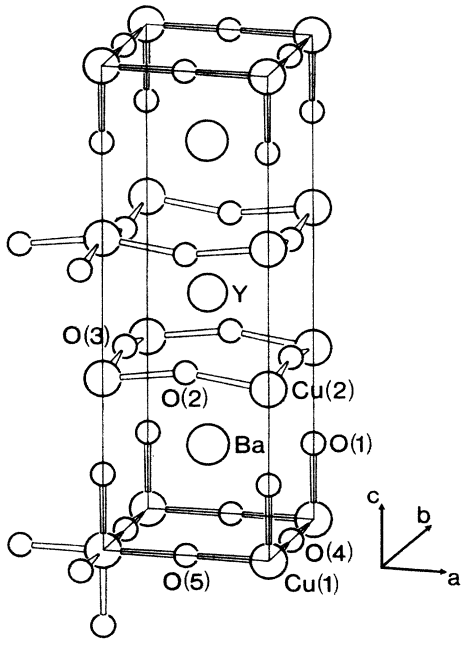

FIG. 1. Unit cell of orthorhombic $Ba_2YCu_3O_{8-\delta}$.

ically equivalent if the structure were tetragonal, also differ by only 0.06 Å.

In an earlier publication we reported the first determination by single-crystal neutron diffraction of a tetragonal nonsuperconducting phase with $\delta = 1.74$.[14] The major structural differences between the tetragonal and orthorhombic phases are the equal (partial) occupations of the O(4) and O(5) sites and a lengthening of the c axis in the tetragonal phase, the latter primarily due to an increase in the Ba-Ba separation which arises from an increase in the Ba^{2+}-Ba^{2+} repulsion by the decrease in the oxygen occupation in the $z = 0$ plane. Our tetragonal sample had been obtained by rapid quenching of the crystal from high temperature. More recently Jorgensen *et al.*[15] have demonstrated in an extensive temperature-dependent study that the transition from the orthorhombic to the tetragonal structure occurs for $\delta \simeq 1.5$, and, under equilibrium conditions, at temperatures up to 700 °C, the exact temperature of the transition depending on the oxygen partial pressure. They also observed that the disordering of the oxygen on O(4) and O(5) occurs continuously as the transition to the tetragonal phase is approached. The O(5) site appears to be completely vacant only below about 400 °C for samples that are annealed and slowly cooled. From simple charge balance considerations, $\delta = 1.5$ corresponds to the oxygen concentration at which the average Cu charge state is 2+. It has been supposed that the depression or absence of the superconducting transition temperature in quenched tetragonal samples[16,17] could be due either to the disorder of the oxygen atoms which breaks up the CuO_4 chains, or to the absence of Cu^{3+} ions.[15,18] The occurrence of superconductivity near 90 K in $Ba_2EuCu_3O_{8-\delta}$, which is isostructural with the tetragonal phase of $Ba_2YCu_3O_{8-\delta}$,[19] tends however to discount the former supposition. In addition, the superconducting transition temperature in $Ba_2Y(Cu_{1-x}M_x)_3O_{8-\delta}$ is unaffected by the orthorhombic-to-tetragonal transition induced by the impurities M = Fe, Co, Ni, Zn, and Ga.[20]

One aim of the many diffraction investigations of the superconducting phase has been to search for any structural change associated with the superconducting transition. Understandably the first investigations were made with the more readily accessible, quicker techniques, x-ray diffraction and then neutron powder diffraction. However none of these studies has thus far revealed any structural anomalies in orthorhombic $Ba_2YCu_3O_{8-\delta}$ between 10 K and room temperature. The dynamic behavior of the atoms in the CuO_4 chains was thought to play a key role in the existence of superconductivity, but the only features of note observed are unusually large thermal vibrations of the atom at the site O(4) over the whole temperature range.[8] While neutron powder diffraction offers some advantages over x-ray methods with regard to determination of the oxygen parameters in this structure, the greatly improved reflection-resolving power of single-crystal neutron diffraction makes it the preferred technique, provided suitably large crystals can be grown. Since the crystalline material is prepared by sintering near 900 °C, the as-grown structure is tetragonal. When cooled into the orthorhombic phase the single crystals necessarily exhibit twinning in the absence of an external uniaxial force.[16]

In this paper we report the first investigation by single-crystal neutron diffraction of the domain and crystal structure of the orthorhombic phase above and below the superconducting transition temperature. To effect some separation of the individual orthorhombic reflections, the data were recorded using a multidetector. The effect on the twinned and untwinned structure factors of the relative oxygen occupation of the O(4) and O(5) sites is considered in detail.

II. EXPERIMENT

A powder sample with Y:Ba:Cu composition ratio 1:2:3 was prepared by reaction in air of stoichiometric proportions of Y_2O_3, $BaCO_3$, and CuO at 950 °C. The reaction product was confirmed to be single phase by x-ray diffraction on a Guinier-Laine camera. Small single crystals with well-defined faces were obtained by long annealing of the powder in air at about 900 °C, followed by quenching to room temperature. One of these crystals was selected for the previously reported study of the tetragonal phase.[14] A number of the remaining crystals were reheated to 800 °C in an oxygen atmosphere, and cooled slowly to room temperature. This treatment caused significant degradation of the definition of the crystal faces and, in many cases, of the single-crystal quality of the bulk. The first three crystals inspected on the diffractometer gave diffraction patterns similar to those from coarse-grained powders. Only the fourth crystal, which had similarly poor definition of the crystal faces as the first three, gave Bragg peaks with intensity expected for this size sample. This sample, which was nearly cubic in shape, approximately 0.5 mm along each edge, was used for the neutron diffraction measurements.

The diffraction data were collected on the four-circle multidetector diffractometer D19 on the H11 thermal neutron beam at the Institut Laue-Langevin.[21] The detector is a gas-filled two-dimensional multiwire proportional counter, 8 cm wide and curved along its height of 128 cm.[22] The spacings of the horizontal anodes and vertical cathodes are 2.54 mm and 5.00 mm, respectively; the sample-to-detector distance is approximately 1160 mm. These spacings correspond to pixel separations of 0.125° vertically and 0.25° horizontally subtended at the sample. The crystal was mounted in an Air Products two-stage Displex cryorefrigerator.

Two sets of measurements were made. For the first, a wavelength of 1.3188 Å obtained by reflection from the (115) planes of a vertically focusing Ge monochromator was used. The choice of a relatively long wavelength for such a small unit cell was a compromise between the need for high flux for the abnormally small crystal volume and the desirability of data at high $(\sin\theta)/\lambda$. Because of the small ratio of unit-cell dimensions to wavelength, the data were collected in equatorial-plane geometry. All reflections in a quadrant of reciprocal space to $(\sin\theta)/\lambda = 0.68$ Å^{-1} were scanned at 40 and 100 K.

For the second set of measurements, a wavelength of 2.41 Å obtained by reflection from the (002) planes of a

flat highly oriented pyrolytic graphite monochromator was used. This wavelength was chosen to give the highest flux at the sample and the largest radial resolution is reciprocal space. 20′ Soller slits were placed in the primary beam just after the monochromator to improve the resolution at Bragg angles beyond the focusing angle of the monochromator. Again the reflections were scanned in equatorial-plane geometry. Only a few reflections were scanned, mainly the 010 with c^* perpendicular to the plane of diffraction and $\bar{1}00$ and $\bar{1}03$ both with b^* nearly perpendicular to the plane of diffraction, at a number of temperatures from 40 to 150 K.

III. OBSERVATIONS AND DATA REDUCTION

A. Full data collection at 1.3188 Å

At both temperatures it was apparent from the rocking curves that the crystal was multidomained, and that the multiple peaks in each scan were to a reasonable approximation centered on a tetragonal reciprocal lattice. One advantage of a two-dimensional position-sensitive detector is that under favorable conditions it allows a three-dimensional mapping of reciprocal space about each reflection. In the present case, however, the monochromator, focused on the sample in the vertical plane, broadens the diffracted beam too much in the vertical direction to allow unambiguous identification of the reflections from different domains in that direction. The best resolution is obtained in the projection of the count distribution onto the equatorial plane. In Fig. 2 we present the projection onto the $\omega-2\theta$ plane of the count distribution observed for the 006 reflection at 100 K. In this case, one of the tetragonal basal-plane axes is approximately perpendicular to the equatorial plane, but the same distribution is also observed for this reflection for other orientations of the axes. This and other $\{00l\}$ reflections are clearly single. By contrast the $\{0k0\}$ reflections shown in Fig. 3 are not. For these scans c^* is approximately vertical. In general four peaks are observed around each tetragonal reciprocal lattice point, although only the pair at the same 2θ are of equal intensity. By transforming the observed peak centers from instrumental coordinates to reciprocal lattice coordinates the peaks may be indexed with respect to the average tetragonal lattice. We find that the four peaks lie very nearly at the corners of a square centered on

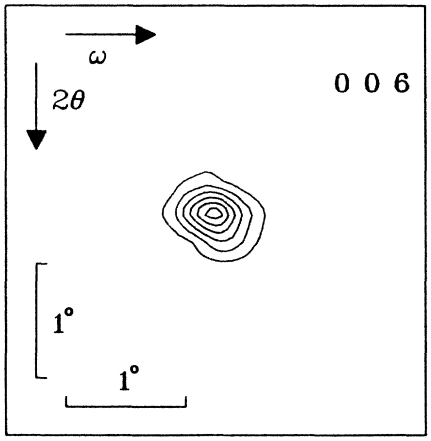

FIG. 2. Projection onto the ω-2θ plane of the count distribution observed in the 006 scan at 100 K and $\lambda = 1.3188$ Å.

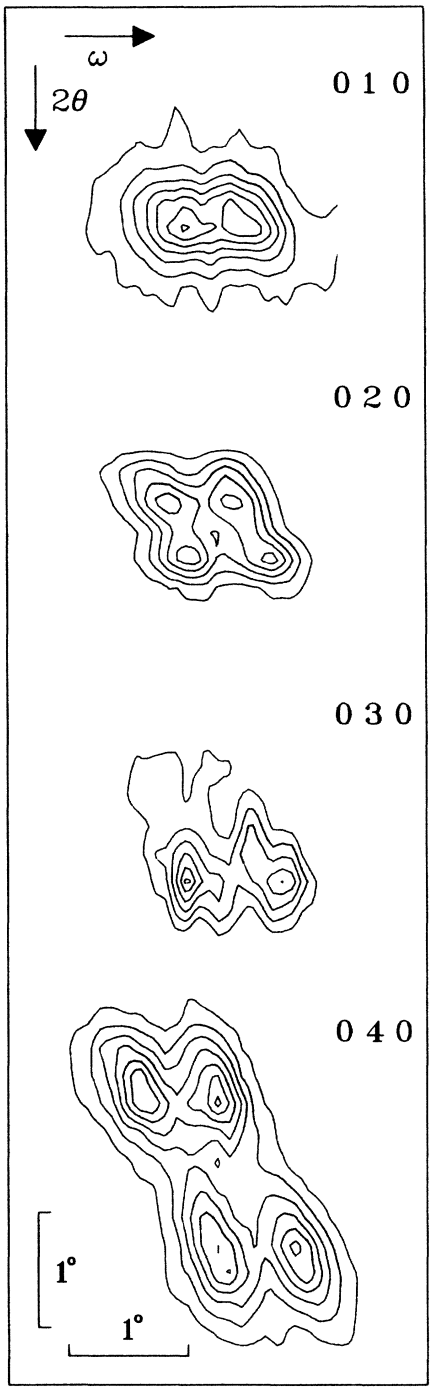

FIG. 3. Projection onto the ω-2θ plane of the count distribution observed in scans through various $\{0k0\}$ reflections at 100 K and $\lambda = 1.3188$ Å. The distribution in ω and 2θ is related to the distribution in reciprocal space by a homogeneous affine transformation for small $\Delta\omega$ and $\Delta 2\theta$ (Ref. 31).

the tetragonal reciprocal lattice point and aligned along the tetragonal axes. The size of the square is proportional to the length of the reciprocal lattice vector. Similar distributions are observed for the $\{h00\}$ reflections. Supposing an orthorhombic unit cell for a single domain we can construct the expected diffraction pattern in reciprocal space for each layer of constant l (Fig. 4). Reflections hkl with at least one of h and k nonzero with $|h| \neq |k|$ are quadruply split, while reflections with $|h| = |k| \neq 0$ are triply split. This was later confirmed by inspection of the three-dimensional distributions around a number of reflections in each class (Fig. 5). The same diffraction pattern has been observed by x-ray precession photography.[16,23]

The quadruple splitting of the reflections may be explained if one considers the likely response of the crystal as it is cooled from the tetragonal phase to the orthorhombic phase. As the crystal passes through the transition neither of the tetragonal-basal plane axes is privileged to become the shortest orthorhombic axis. On average it will just as frequently be one axis as the other . The macroscopic translational symmetry of the initial tetragonal phase will constrain the orientations of the two groups of orthorhombic domains to be 90° to one another (Fig. 6). At the microscopic level, however, the near equivalence of the two shorter orthorhombic axes and the mirror equivalence of the orthorhombic cell across the planes normal to (110) and ($\bar{1}$10) allow local twinning with an angle of $2\tan^{-1}(b/a)$ between the orthorhombic a axes of the two orientations (Fig. 7).[24] The twinning could occur across both the (110) and the ($\bar{1}$10) planes, but to maintain the microscopic translational symmetry the twinning in any one crystal grain will be across just one set of planes. The twinning within a single grain is readily observed by electron diffraction.[24,25] While either orientation of the twin planes in a particular grain is equally likely if the grain is considered in isolation, one orientation will be preferred to maintain the macroscopic translational symmetry of the crystal. Hence only a quadrupling of the orthorhombic reciprocal lattice over the whole crystal is observed. Thus we obtain the diffraction pattern of Fig. 4. Comparison of the intensity distributions in the $\{h00\}$

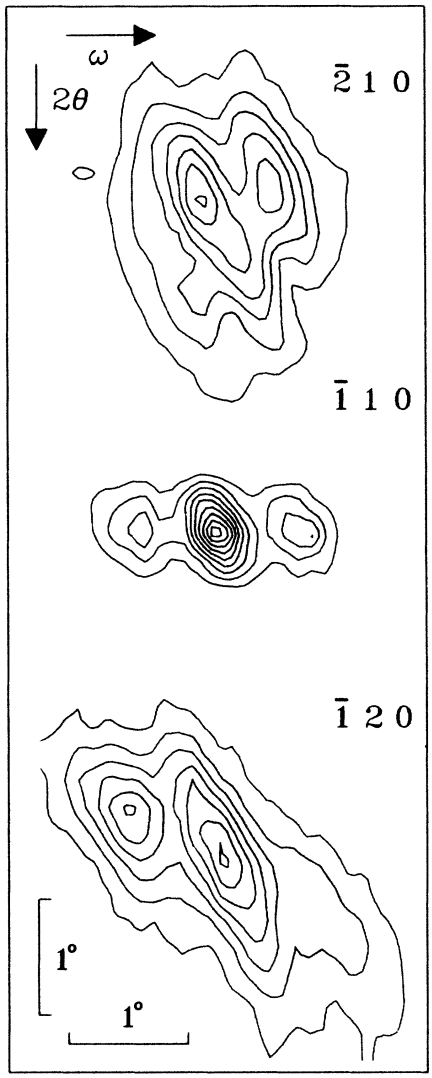

FIG. 5. Projection onto the ω-2θ plane of the count distribution observed in $\bar{2}10$, $\bar{1}10$, and $\bar{1}20$ scans at 100 K and $\lambda = 2.41$ Å.

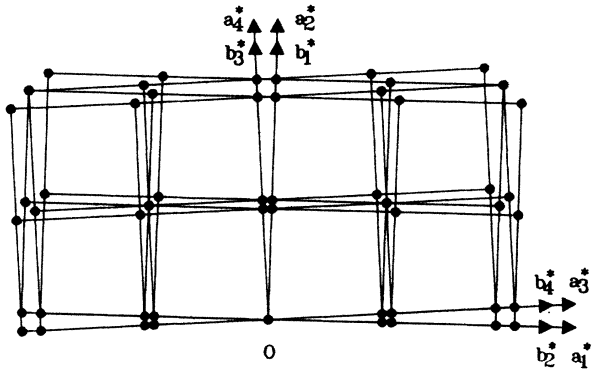

FIG. 4. Schematic of the observed reciprocal lattice of orthorhombic $Ba_2YCu_3O_{8-\delta}$ in planes of constant l. Four orientations of the orthorhombic reciprocal cell are observed denoted by $a_i^* b_i^*$ ($i = 1$ to 4).

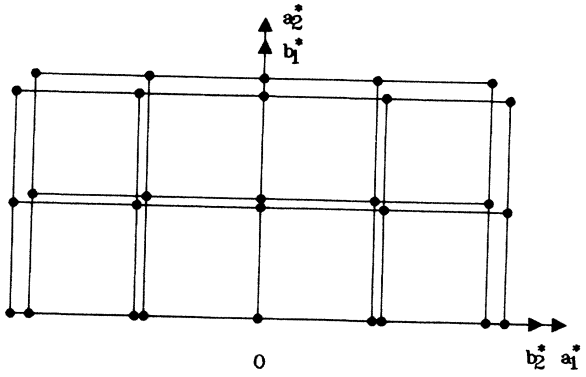

FIG. 6. Doubling of the reciprocal lattice due to macroscopic twinning.

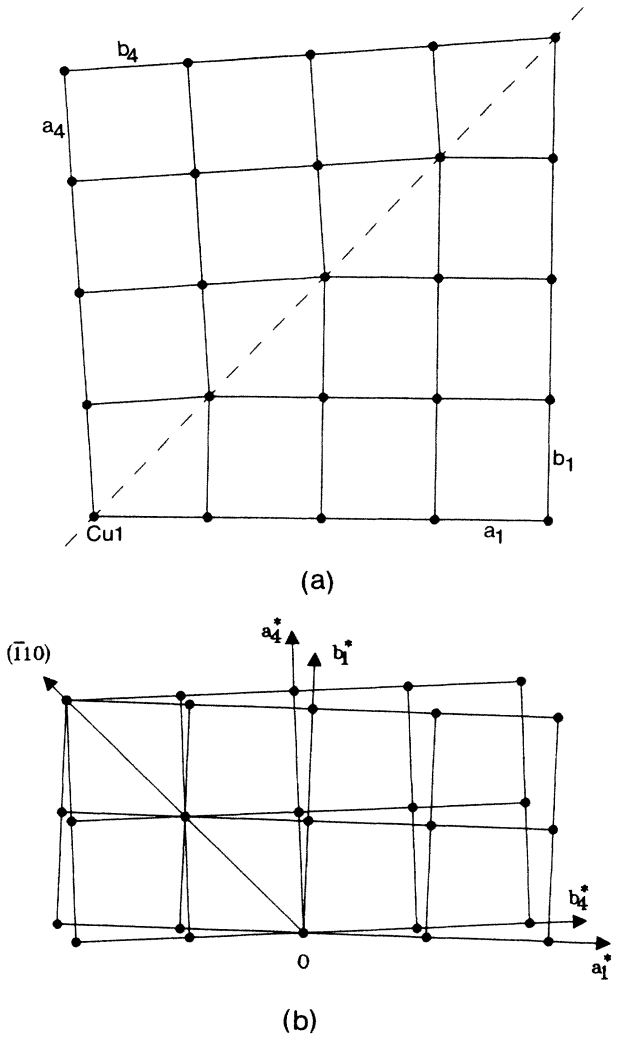

FIG. 7. (a) Twinning of the real space lattice about (110). (b) Doubling of the reciprocal lattice corresponding to the microscopic twinning in (a) a_1^* makes an angle $2\tan^{-1}(b/a)$ to a_4^*. $a_2^*b_2^*$ and $a_3^*b_3^*$ are similarly related.

and $\{0k0\}$ scans shows clearly that the fraction of the crystal in each orientation is the same. The diffraction pattern has $4/mmm$ Laue symmetry.

From Fig. 4 it is the $\{h00\}$ and $\{0k0\}$ reflections which for a favorable choice of rotation axis will show the best resolution of the four peaks, and even then the peaks overlap to some extent (Fig. 3). In the first reduction of the data we therefore attempted simply to integrate over all four peaks in each scan. In view of the very small crystal size by normal neutron diffraction standards, optimization of the accuracy of the structure factors is essential. For single-domain, small-mosaic samples the three-dimensional array of counts observed around each scanned reflection on D19 is usually corrected for background and reduced to squared structure amplitudes by using the three-dimensional integration method of Wilkinson and Khamis.[26] Unfortunately this method in its present implementation is not entirely appropriate to the integration of reflections whose extent depends not only on the instrumental resolution, but also on the anisotropic crystal mosaic structure.

Following the method of Wilkinson and Khamis the limit to the peak extent for strong reflections was found by reference to the ellipsoidal surface for which $\sigma(I)/I$, where I is the background-corrected sum of the counts within the ellipsoid and $\sigma(I)$ is the estimated error in I due to counting statistics, is a minimum. The shape and orientation of the ellipsoid are found from the moment-of-inertia tensor of the (unit-weighted) stronger peak counts. For our sample and resolution function an enlargement by a factor 4 of the volume which gave the minimum $\sigma(I)/I$ was found to contain all the peak counts for the strong peaks. The choice of an ellipsoidal volume of integration for reflections that are multipeaked decreases only the precision of the reduced squared structure amplitude; included within the ellipsoid are background points that might otherwise be excluded from a volume whose surface more closely models the distribution.

Normally the ellipsoid parameters for weak peaks would be deduced by interpolation amongst the values for strong peaks at the same 2θ. This is inappropriate in our case since the extent of our peaks depends on the orientation of the reciprocal lattice as well as 2θ. The weak peaks were therefore integrated simply by summing the counts within the ellipsoid which was known to encompass all the peak counts for all strong peaks. The precision of the reduced squared structure amplitudes for the weak peaks is lowered by comparison to the strong peaks, but at least systematic errors are avoided by this method.

Because of the very small crystal size corrections for sample absorption and extinction were unnecessary. At both temperatures the integrated intensities were averaged according to the Laue class $4/mmm$. The agreement indices in the averaging are given in Table I.

The splitting of the reflections in both ω and 2θ complicates the determination of the cell parameters. The integration method of Wilkinson and Khamis gives the observed instrumental coordinates of the center of the (unit-weighted) moment-of-inertia tensor of the peak counts. Since the diffraction pattern has tetragonal symmetry, refinement of the cell parameters against these coordinates gives only the average tetragonal cell. The basal plane axes refined from the centers of the approximately 200 stronger reflections scanned at 40 and 100 K were 3.8523(5) Å and 3.8553(5) Å, respectively. The unique c axes which are unaffected by the orthorhombic splitting are given in Table I. To obtain the orthorhombic cell parameters we must determine the centers of the individual peaks. The best resolved strong peaks are those in the scans through the $\bar{4}00$ and the 040. To determine the instrumental coordinates of the individual peaks the ω-2θ projections of the three-dimensional count distribution of each scan were fitted by two or four two-dimensional Gaussian peaks in the manner described by McIntyre and Visser.[27] The corresponding width parameters for all peaks in the one scan were constrained to be equal. The observed and fitted distributions for the $\bar{4}00$ and 040 scans at 100 K are shown in Fig. 8. From the difference in the refined (fractional) cathode values of the centers of the

TABLE I. Lattice parameters and refined fractional atomic coordinates, occupation factors, and thermal parameters for orthorhombic $Ba_2YCu_3O_{6.70}$. The atomic parameters of O(3) are constrained to be related by tetragonal symmetry to those of O(2). The anisotropic temperature factor has the form $\exp(-h^2B_{11}/4a^2-k^2B_{22}/4b^2-l^2B_{33}/4c^2)$, where the units of the B_{ij} are Å^2. The residuals are

$$R_{\text{merge},w}(F^2)=\left[\sum[1/\sigma^2(F_o^2)](F_o^2-\langle F\rangle^2)^2/\sum[1/\sigma^2(F_o^2)]F_o^4\right]^{1/2},$$

$$X_{\text{merge}}=\left[(1/n)\sum[1/\sigma^2(F_o^2)](F_o^2-\langle F\rangle^2)^2\right]^{1/2},$$

$$R(F)=\sum|F_o-F_c|/\sum F_o,$$

$$R_w(F)=\left[\sum[1/\sigma^2(F_o)](F_o-F_c)^2/\sum[1/\sigma^2(F_o)]F_o^2\right]^{1/2},$$

$$\chi=\left[\sum[1/\sigma^2(F_o)](F_o-F_c)^2/(n-p)\right]^{1/2},$$

where F_o and F_c are the observed and calculated structure factors, $\langle F\rangle$ is the average of the set of equivalents to F_o, n is the number of observations, and p is the number of parameters.

		Temperature (K) 40	100
	a	3.8273(5)	3.8303(5)
	b	3.8773(5)	3.8803(5)
	c	11.6548(13)	11.6669(13)
	V	172.95	173.40
Ba	z	0.1865(4)	0.1868(5)
	B_{11}	0.72(11)	0.89(16)
	B_{33}	0.72(13)	0.71(18)
Y	B_{11}	0.76(11)	0.93(16)
	B_{33}	0.56(14)	0.63(19)
Cu(1)	B_{11}	1.02(13)	1.36(19)
	B_{33}	0.74(15)	0.48(19)
Cu(2)	z	0.3557(3)	0.3555(3)
	B_{11}	0.69(7)	0.68(10)
	B_{33}	0.47(9)	0.51(12)
O(1)	g	0.96(2)	0.94(3)
	z	0.1577(4)	0.1577(5)
	B_{11}	1.24(13)	1.19(19)
	B_{33}	0.50(18)	0.83(24)
O(2)	g	0.98(2)	0.98(2)
	z	0.3780(2)	0.3783(2)
	B_{11}	0.58(11)	0.62(15)
	B_{22}	0.80(11)	0.96(16)
	B_{33}	0.50(11)	0.57(14)
O(4)	g	0.77(2)	0.76(2)
	B_{11}	1.8(5)	1.5(7)
	B_{22}	0.3(4)	0.9(6)
	B_{33}	0.2(3)	0.5(4)
No. of reflections scanned		458	523
$R_{\text{merge},w}(F^2)$		5.4%	6.8%
χ_{merge}		1.62	1.73
No. of unique reflections		181	182
$R(F)$		6.5%	8.2%
$R_w(F)$		5.4%	7.1%
χ		1.63	2.00

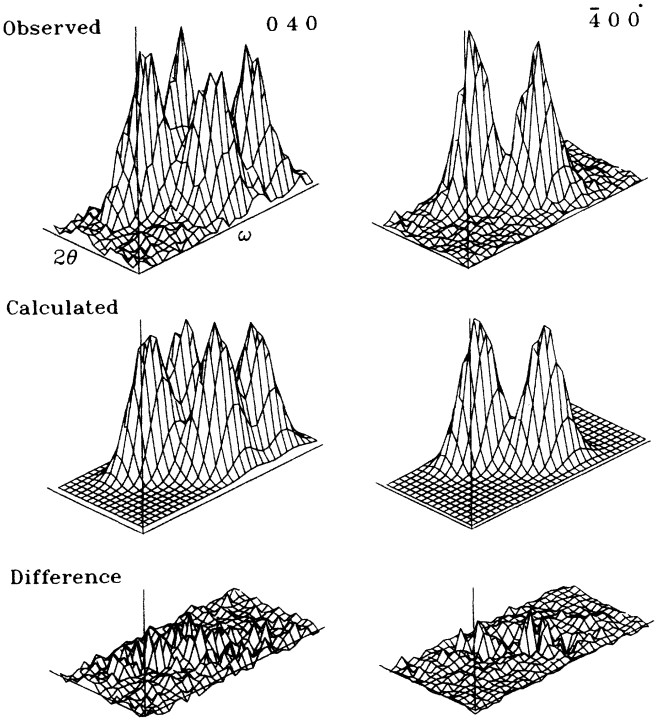

FIG. 8. Observed and fitted projections onto the ω-2θ plane of the multiple peaks in (a) the 040 scan and (b) the $\bar{4}00$ scan, both at 100 K with $\lambda=1.3188$ Å.

peaks at different 2θ, we can derive the difference in the orthorhombic a and b axes. At both 40 and 100 K the difference is 5.54(8) cathodes for the $\bar{4}00$ and 040 reflections both of which occur at $\theta\simeq 43°$. The corresponding difference in cell parameters is 0.050(1) Å. From this difference and the average tetragonal cell parameter we arrive at the cell parameters given in Table I.

B. Limited data collection at 2.41 Å

The scans 010, $\bar{1}00$, and $\bar{1}03$ had been chosen as those which, as discussed below, should show the greatest difference in intensity between the two pairs of orthorhombic peaks in the scan. For the 010 scan, with c^* perpendicular to the plane of diffraction, four peaks should be observed in the projection of the count distribution onto the ω-2θ plane, while for the $\bar{1}00$ and $\bar{1}03$ scans, which have b^* perpendicular, only two peaks should be observed. Despite the long wavelength and the use of Soller slits only the $\bar{1}03$ scans displayed clearly identifiable peaks at different 2θ values. The ω-2θ projections of the $\bar{1}03$ scans were fitted to a pair of two-dimensional Gaussian peaks. Again corresponding width parameters for the two peaks were constrained to be equal. The observed and final fitted distributions for the scan at 100 K are shown in Fig. 9.

The quantity of interest from these fits is the ratio of the squared structure amplitudes of the nonequivalent orthorhombic reflections, given by the ratio of the volumes of the two peaks in the ω-2θ projection. Since the width

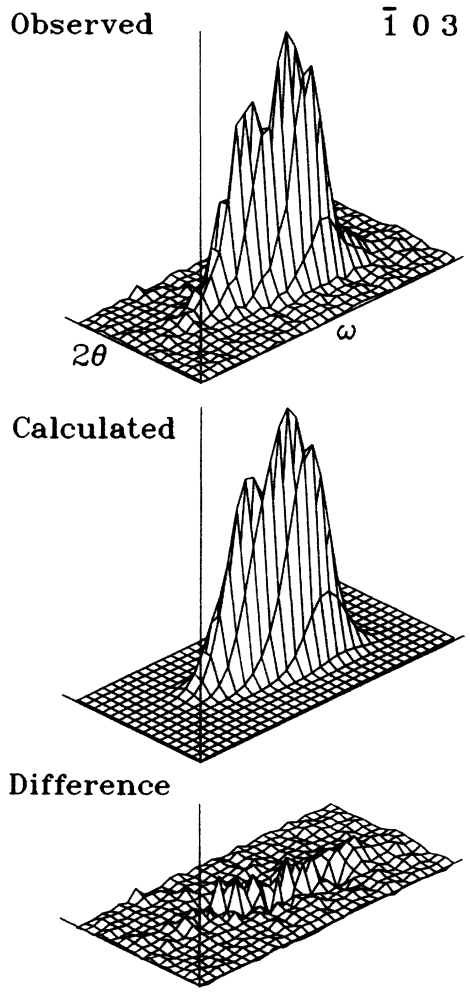

FIG. 9. Observed and fitted projection onto the ω-2θ plane of the multiple peaks in the $\bar{1}03$ scan at 100 K with $\lambda = 2.41$ Å.

parameters are constrained to be equal, this is equal to the ratio of the peak heights. Within error the ratio remained constant from 40 to 150 K, the values at 40 and 100 K being 1.49(8) and 1.38(8), respectively.

IV. STRUCTURE

Refinements were carried out in the orthorhombic space groups *Pmm*2, *P*222, and *Pmmm*, using the full-matrix least-squares refinement program UPALS,[28] modified to allow for twinning of the orthorhombic cell to give a tetragonal diffraction pattern. Initial atomic positions were taken from the results of Siegrist *et al.*[5] The observed structure amplitude is compared to the domain averaged calculated amplitude $F_c'(hkl)$, which is given in terms of the calculated amplitudes for one domain, $F_c(hkl)$, by

$$[F_c'(hkl)]^2 = \tfrac{1}{2}[F_c^2(hkl)+F_c^2(khl)] \ . \qquad (1)$$

The refinements in the lower-symmetry space groups *Pmm*2 and *P*222 did not significantly improve the agreement compared with refinement in the highest-symmetry space group, despite having larger numbers of adjustable parameters. We therefore discuss only the results of the refinements in *Pmmm*, $Z=1$ with Ba at the Wyckoff positions 2t($\frac{1}{2},\frac{1}{2},z$), Y at 1h($\frac{1}{2},\frac{1}{2},\frac{1}{2}$), Cu(1) at 1a(0,0,0), Cu(2) at 2q(0,0,z), O(1) at 2q(0,0,z), O(2) at 2s($\frac{1}{2}$,0,z), O(3) at 2r(0,$\frac{1}{2}$,z), O(4) at 1e(0,$\frac{1}{2}$,0), and O(5) at 1b($\frac{1}{2}$,0,0).

Since the oxygen occupations appear to play a key role in the superconductivity, and may be determined to relatively high precision from neutron data, we allowed them all to vary. The temperature factors for all atoms were allowed to be anisotropic in the final refinements. The pseudotetragonal arrangement of the oxygen atoms leads to high correlation between corresponding refined parameters for O(2) and O(3), between the thermal parameters of O(4) and O(5), and between B_{11} and B_{22} for the atoms situated on the pseudotetragonal axis (B_{ij} is defined in Table I). This is accentuated by the form of the twinned structure factor $F_c'(hkl)$. It was therefore necessary to constrain all parameters except the O(4) and O(5) occupations to be related by tetragonal symmetry, i.e., B_{11} is equal to B_{22} for Ba, Y, Cu(1), Cu(2), and O(1), the z coordinates of O(2) and O(3) are equal, and B_{11} of O(2) and O(3) are equal *and* equal to B_{22} for the same atoms. Similarly B_{11} and B_{22} for sites O(4) and O(5) are equal.

At both temperatures the refinement converged rapidly to nearly complete occupation of the sites O(1), O(2), and O(3), and to a total absence of oxygen in the $z=\frac{1}{2}$ plane. Refinement of the occupancy of the sites O(4) and O(5) gave, respectively, 67(5)% and 12(5)% at 40 K, and 60(5)% and 25(5)% at 100 K. The seemingly significant disordered occupation of *both* the O(4) and O(5) sites, particularly at 100 K, is curious, especially in view of the complete absence of oxygen observed at this site below 400 K by neutron powder diffraction.[8-13] Before we attribute physical significance to this result however we should consider in detail the effect of the relative occupations of the O(4) and O(5) sites on the tetragonally averaged structure factors that have been used in these refinements.

Trial calculations of the expected structure factor were made for a tetragonal structure with 50% occupation of both sites, for an orthorhombic structure with full occupation of O(4) and O(5) vacant, and for the same orthorhombic structure twinned to give a tetragonal diffraction pattern. These showed that reflections with $h+k=2n$ are virtually the same for all three models. For reflections with $h+k=2n+1$ the orthorhombic structure factors differ markedly from the tetragonal and the twinned orthorhombic structure factors, while the latter two are similar. Thus the 020 and 040 scans in Fig. 3 show four peaks of nearly equal height, while for the 010 and 030 scans two peaks are much stronger. The lack of sensitivity of the twinned structure factor to the relative occupation of O(4) and O(5) is not surprising if we consider the analytical contribution of these two sites to the untwinned orthorhombic structure factor. This contribution is $bTg_{O(4)}\cos(\pi k)+bTg_{O(5)}\cos(\pi h)$, where b is the neutron scattering length for oxygen, T is the thermal factor assumed to be the same for both atoms, and g_j is the occupation of the site j. For $h+k=2n$ the contribution be-

comes $\pm bT(g_{O(4)}+g_{O(5)})$, while for $h+k=2n+1$ it is $\pm bT(g_{O(4)}-g_{O(5)})$. Only in the latter case is the contribution sensitive to the relative occupations of O(4) and O(5). For reflections with $h+k=2n+1$ from the twinned orthorhombic structure, the squared structure amplitude $[F_c'(hkl)]^2$ [Eq. (1)] will contain a term $+bT(g_{O(4)}-g_{O(5)})$ in one of the domain contributions and a term $-bT(g_{O(4)}-g_{O(5)})$ in the other domain contribution. The two contributions will tend to cancel one another. The largest difference between untwinned orthorhombic structure factors is shown by the reflections with $h+k=2n+1$. Considering the further decrease in intensity with increasing Bragg angle, the difference should be most readily observable in low Bragg-angle reflections such as 100 and 103.

To test the sensitivity of the refinement to the relative occupations of O(4) and O(5) we performed a series of refinements in which the occupation of O(5) was fixed at values from 0 to 80% [80% is the sum of the O(4) and O(5) occupations when refined independently]. The results of this test for the 100 K data are shown in Fig. 10 where we plot the weighted R factor against the fixed O(5) occupation. For comparison we also plot the calculated twinned orthorhombic structure factor for the 103 reflection, and the ratio of the untwinned orthorhombic structure factors 103 and 013. Clearly the twinned structure factor and the R factor are nearly insensitive to the occupation ratio. On the other hand, the ratio of the untwinned reflections, if it could be measured, would be a very sensitive indicator of the relative occupations of the O(4) and O(5) sites.

It was this last observation that prompted us to perform slow scans through the 100 and 103 reflections at the longer wavelength of 2.41 Å (see Sec. III B). As noted above only the 103 scans clearly exhibited two peaks in the 2θ direction. (This is one area where powder diffractometry with its usually better resolving power in 2θ affords an advantage over single-crystal diffractometry.) In Fig. 10 are also marked the intensity ratios of the orthorhombic pair observed in the $\bar{1}03$ scans at 40 and 100 K in the second experiment. It is clear that the site O(5) is completely vacant at both temperatures. Therefore O(5) was omitted from all further refinements.

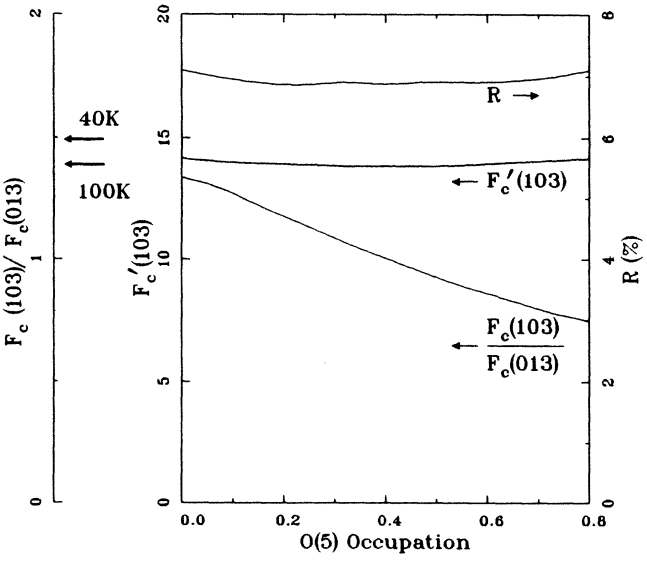

FIG. 10. Results of test refinements on the 100 K data. The weighted R factor, the twinned orthorhombic structure factor $F_c'(103)$, and the ratio of the individual orthorhombic structure factors $F_c(103)/F_c(013)$ vs percentage occupation of the O(5) site. The arrows denote the observed ratios at 40 and 100 K.

Large thermal parameters were observed for Cu(1), O(1), and O(4). For O(4) the largest parameter corresponds to motion perpendicular to the common plane of Cu(1), O(1), and O(4) (i.e., along a). Unfortunately we cannot say if this is also the case for Cu(1) and O(1) due to the need to constrain B_{11} to be equal to B_{22} for these atoms. We do not observe the unusually large values of B_{33} for O(4) that were reported in the powder studies.[8,11] A further remark concerning the thermal parameters of O(4) should also be made. The very large value of B_{11} observed for O(4) could also indicate static disorder in the position of O(4). In principle, static and dynamic disorder may be distinguished by extrapolation of plots of the mean square displacements (derived from the B_{ij}) versus temperature to 0 K. However, the uncertainties on the thermal parameters obtained in this experiment are too large to allow a definite statement of the origin of the large thermal parameters of Cu(1), O(1), and O(4) to be made. Clearly more precise diffraction data to a higher $(\sin\theta)/\lambda$ limit are needed, preferably on an untwinned crystal.

The final refined atomic coordinates at 40 and 100 K are given in Table I. At both temperatures the refinements indicated less than full occupation of the O(1), O(2), and O(3) sites, and the refined occupations are given in Table I. We note however that assuming full occupation of these sites did not increase the R factor, nor alter the other refined parameters significantly. The refined oxygen occupancies correspond to the composition $Ba_2YCu_3O_{6.70}$ within error at both temperatures. No significant differences in the atomic positions are observed between 40 and 100 K. The agreement between the atomic positions at the two temperatures and the consistency of the increase in the thermal parameters from 40 to 100 K,

TABLE II. Selected interatomic distances (Å) in orthorhombic $Ba_2YCu_3O_{8-\delta}$, determined in this study at 40 and 100 K, and by neutron powder diffraction at 30 K (Ref. 8).

	Number of distances	Temperature (K) 40	100	30
Ba-O(1)	4	2.745(1)	2.747(1)	2.734(1)
Ba-O(2)	2	2.957(4)	2.959(5)	2.971(4)
Ba-O(3)	2	2.941(5)	2.943(5)	2.957(4)
Ba-O(4)	2	2.897(4)	2.901(4)	2.854(4)
Y-O(2)	4	2.405(2)	2.404(2)	2.415(2)
Y-O(3)	4	2.385(2)	2.384(2)	2.381(2)
Cu(1)-O(1)	2	1.840(5)	1.840(6)	1.855(5)
Cu(1)-O(4)	2	1.9386(1)	1.9402(1)	1.940(0)
Cu(2)-O(1)	1	2.307(6)	2.308(7)	2.269(4)
Cu(2)-O(2)	2	1.931(1)	1.933(1)	1.925(1)
Cu(2)-O(3)	2	1.956(1)	1.958(1)	1.958(1)

are as good as or better than observed in the multitemperature powder studies,[8-10] despite the generally larger estimated standard deviations in our case. The distances between the heavy atoms and the oxygen atoms are given in Table II. The Cu(2)-Cu(2) distance is clearly too short to accommodate an oxygen atom at $z = \frac{1}{2}$ as proposed by Reller, Bednorz, and Müller.[29] As the comparison in Table II shows, we obtained essentially the same atomic positions as by neutron powder diffraction.

V. CONCLUSION

The domain and crystal structure of the superconducting orthorhombic phase $Ba_2YCu_3O_{8-\delta}$ ($\delta \simeq 1.30$) has been investigated for the first time by single-crystal neutron diffraction.

As the crystal is cooled from the tetragonal phase the reciprocal lattice points will in general be quadruply split parallel to the tetragonal basal plane. Two domain orientations occur due to interchange of the orthorhombic a and b axes at the macroscopic level; for each orientation microscopic twinning across either the (110) or ($\bar{1}$10) planes can occur, the choice of planes being determined by the macroscopic translational symmetry.

Refinement of the O(4) and O(5) oxygen occupations against the observed twinned orthorhombic structure factors is rather insensitive, and some separation of the untwinned structure factors is necessary. By fitting the multipeaked ω-2θ projections of the three-dimensional count distributions recorded by a multidetector in the vicinity of the reflections we could determine some untwinned structure factors and show that only the O(4) site is occupied.

Particularly large thermal parameters were observed for Cu(1), O(1), and O(4). Unfortunately, the temperature-dependent data are not precise enough to distinguish between static and dynamic disorder. Now that large single crystals can be grown,[30] it is feasible to collect accurate neutron data at shorter wavelengths and thereby to a higher $(\sin\theta)/\lambda$ limit to yield more detailed information on the vibrational behavior. In such an experiment it would be necessary to resolve the individual orthorhombic reflections, either by selection of an untwinned crystal, or by extension of the analysis performed here, in order to determine orthorhombic thermal ellipsoids of vibration for atoms besides O(2), O(3), and O(4).

ACKNOWLEDGMENTS

We gratefully acknowledge the particular support of the directors of the Institut Laue-Langevin for this work. We especially thank Professor J. Lajzerowicz-Bonneteau for sage counsel on all aspects of the refinements. We also wish to thank Dr. Sax Mason for his considerable advice, Mr. Michel Berneron for technical assistance during the experiment, and Dr. J.-P. Pouget and Dr. R. Comès for constructive discussions.

---

*Present address: The Studsvik Neutron Research Laboratory, University of Uppsala, 61182 Nyköping, Sweden.

†Permanent address: Laboratoire de Spectrometrie Physique, Université Scientifique Technologique et Médicale de Grenoble, BP 87, 38402 Saint Martin d'Hères, France.

[1] M. K. Wu, J. R. Ashburn, C. J. Torng, P. H. Hor, R. L. Meng, L. Gao, Z. J. Huang, W. Q. Wang, and C. W. Chu, Phys. Rev. Lett. **58**, 908 (1987).

[2] C. N. R. Rao, P. Ganguly, A. K. Raychaudhuri, R. A. Mohan Ram, and K. Sreedhar, Nature **326**, 856 (1987).

[3] D. G. Hinks, L. Soderholm, D. W. Capone, J. D. Jorgensen, I. K. Schuller, C. U. Segre, K. Zhang, and J. D. Grace, Appl. Phys. Lett. **50**, 1688 (1987).

[4] G. Bednorz and K. A. Müller, Z. Phys. B **64**, 189 (1986).

[5] T. Siegrist, S. Sunshine, D. W. Murphy, R. J. Cava, and S. M. Zahurak, Phys. Rev. B **35**, 7137 (1987).

[6] R. M. Hazen, L. W. Finger, R. J. Angel, C. T. Prewitt, N. L. Ross, H. K. Mao, C. G. Hadidiacos, P. H. Hor, R. L. Meng, and C. W. Chu, Phys. Rev. B **35**, 7238 (1987).

[7] Y. LePage, W. R. Mckinnon, J. M. Tarascon, L. H. Greene, G. W. Hull, and D. M. Hwang, Phys. Rev. B **35**, 7245 (1987).

[8] J. J. Capponi, C. Chaillout, A. W. Hewat, P. Lejay, M. Marezio, N. Nguyen, B. Raveau, J. L. Soubeyroux, J. L. Tholence, and R. Tournier, Europhys. Lett. **3**, 1301 (1987).

[9] J. E. Greedan, A. H. O'Reilly, and C. V. Stager, Phys. Rev. B **35**, 8770 (1987).

[10] F. Beech, S. Miraglia, A. Santoro, and R. S. Roth, Phys. Rev. Lett. **35**, 8778 (1987).

[11] W. I. F. David, W. T. A. Harrison, J. M. F. Gunn, O. Moze, A. K. Soper, P. Day, J. D. Jorgensen, D. G. Hinks, M. A. Beno, L. Soderholm, D. W. Capone, I. K. Schuller, C. U. Segre, K. Zhang, and J. D. Grace, Nature **327**, 310 (1987).

[12] S. Katano, S. Funahashi, T. Hatano, A. Matsushita, K. Nakamura, T. Matsumoto, and K. Ogawa, Jpn. J. Appl. Phys. **26**, L1046 (1987).

[13] M. A. Beno, L. Soderholm, D. W. Capone, D. G. Hinks, J. D. Jorgensen, I. K. Schuller, C. U. Segre, K. Zhang, and J. D. Grace, Appl. Phys. Lett. **51**, 57 (1987).

[14] A. Renault, G. J. McIntyre, G. Collin, J.-P. Pouget, and R. Comès, J. Phys. (Paris) **48**, 1407 (1987).

[15] J. D. Jorgensen, M. A. Beno, D. G. Hinks, L. Soderholm, K. J. Volin, R. L. Hitterman, J. D. Grace, I. K. Schuller, C. U. Segre, K. Zhang, and M. S. Kleefisch, Phys. Rev. B **36**, 3608 (1987).

[16] P. Strobel, J. J. Capponi, C. Chaillout, M. Marezio, and J. L. Tholence, Nature **327**, 306 (1987).

[17] S. Katano, S. Funahashi, T. Hatano, A. Matsushita, K. Nakamura, T. Matsumoto, and K. Ogawa, Jpn. J. Appl. Phys. **26**, L1049 (1987).

[18] I. K. Schuller, D. G. Hinks, M. A. Beno, D. W. Capone, L. Soderholm, J.-P. Locquet, Y. Bruynseraede, C. U. Segre, and K. Zhang, Solid State Commun. **63**, 385 (1987).

[19] P. H. Hor, R. L. Meng, Y. Q. Wang, L. Gao, Z. J. Huang, J. Bechtold, K. Forster, and C. W. Chu, Phys. Rev. Lett. **58**, 1891 (1987).

[20] Y. Maeno, T. Tomita, M. Kyogoku, S. Awaji, Y. Aoki, K. Hoshino, A. Minami, and T. Fujita, Nature **328**, 512 (1987).

[21] M. Thomas, R. F. D. Stansfield, M. Berneron, A. Filhol,

G. Greenwood, J. Jacobè, D. Feltin, and S. A. Mason, in *Position-Sensitive Detection of Thermal Neutrons,* edited by P. Convert and J. B. Forsyth (Academic, New York, 1983), p. 344.

[22]J. Jacobè, D. Feltin, A. Rambaud, F. Ratel, M. Gamon, and J. B. Pernock, in *Position-Sensitive Detection of Thermal Neutrons,* edited by P. Convert and J. B. Forsyth (Academic, New York, 1983), p. 106.

[23]G. Roth, D. Ewert, G. Heger, M. Hervieu, C. Michel, B. Raveau, F. D'Yvoire, and A. Revcolevschi, Z. Phys. B **69**, 21 (1987).

[24]G. van Tendeloo, H. W. Zandbergen, and S. Amelinckx, Solid State Commun. **63**, 389 (1987).

[25]C. H. Chen, D. J. Werder, S. H. Lion, J. R. Kwo, and M. Hong, Phys. Rev. B **35**, 8767 (1987).

[26]C. Wilkinson and H. W. Khamis, in *Position-Sensitive Detection of Thermal Neutrons,* edited by P. Convert and J. B. Forsyth (Academic, New York, 1983), p. 358.

[27]G. J. McIntyre and D. Visser, J. Phys. (Paris) Colloq. **47**, C5-75 (1986).

[28]J.-O. Lundgren, Institute of Chemistry, University of Uppsala, Sweden, Report No. UUIC-B13-4-05, 1982 (unpublished).

[29]A. Reller, J. G. Bednorz, and K. A. Müller, Z. Phys. B **67**, 285 (1987).

[30]L. F. Schneemeyer, J. V. Waszczak, T. Siegrist, R. B. van Dover, L. W. Rupp, B. Batlogg, R. J. Cava, and D. W. Murphy, Nature **328**, 601 (1987).

[31]A. McL. Mathieson, J. Appl. Crystallogr. **16**, 257 (1983).